Current reversals and current suppression in an open two-degree-of-freedom system

C. Mulhern, D. Hennig, A. D. Burbanks, and A. H. Osbaldestin
Department of Mathematics, University of Portsmouth, Portsmouth, Hampshire, PO1 3HF, United Kingdom
(Received 15 March 2011; published 17 June 2011)

We explore the scattering of particles evolving in a two-degree-of-freedom Hamiltonian system, in which both degrees of freedom are open. Particles, initially having all kinetic energy, are sent into a so-called "interaction region," where there will be an exchange of energy with particles that are initially at rest. The open nature of both components of this system eliminates any restrictions on which particles can escape from the interaction region. Notably, it is shown that two particles can cooperate in a mutual exchange of energy allowing both particles to escape and travel large distances. It is also shown that this level of cooperation is highly sensitive to the coupling strength between both components of the system. Indeed, large fluctuations of the magnitude and direction of the current are observed for small changes of this coupling parameter. Further, it is seen that current reversals are a prominent feature of this model. Another interesting observation is that even with the presence of chaotic scattering, it is possible that the system, for certain parameter regimes, will express a vanishing current, suggesting that there is a restoration of symmetry which, due to the initial setup, is broken. For an explanation of the different features of particle motion, we relate the phase-space dynamics to the various regimes of particle current.

DOI: 10.1103/PhysRevE.83.066207 PACS number(s): 05.45.Ac, 05.60.Cd, 05.45.Pq

I. INTRODUCTION

Transport, and particularly escape phenomena in nonlinear systems, has become a very active research area. Its interest spans many fields and its implications are far reaching. A vast array of application areas lend themselves to be modeled in terms of these systems. Applications include superconductors [1], nanoengines [2], and particle transport in biological systems [3]. This short list is an indication of the breadth of research currently being carried out under the umbrella of transport phenomena in nonlinear systems. In this paper, we investigate particle transport processes modeled by systems of coupled oscillators, evolving in periodic potential landscapes. Two particles will evolve in a so-called "washboard potential" and interact locally with each other via a coupling whose strength strongly influences the dynamics that are seen.

In many systems, the generation of a directed current has been instigated by an external time-dependent field [4–7]. In extended chaotic systems, a nonzero current can be obtained as the time-averaged velocity of an ensemble of trajectories in the chaotic component of phase space and the chaotic transport proceeds ballistically and directedly [7,8]. Once this field is removed or effectively nullified, there is no longer a directed current. Other research has focused on autonomous systems with no external field [9–14]. In these systems, a current is generated through the interaction between various components of the system, and does not rely on a time-dependent external field. A further aspect of current generation is current reversal and this has been examined extensively, particularly in the domain of ratchet potentials [15–17].

In our system, two coupled particles will evolve in a symmetric and periodic washboard potential. Initially, one particle will be sent into the "interaction region," where this particle will interact with another that is initially at rest. (These particles will henceforth be named particle A and particle B, respectively.) The interaction between these particles will be dependent on the strength of coupling between them, and their relative distance from one another. For large distances, the two particles will effectively decouple and individual regular motion will ensue. The objective of this study is to explore the nature of current suppression and reversals of its direction relative to the coupling parameter.

The paper is organized as follows. In Sec. II, we will describe the setup of the system. In addition, we shall show sample trajectories illustrating some of the dynamics present in this model. Particle current is examined in Sec. III. In Secs. IV and V, we examine how long the particles spend in the interaction region, and additionally how energies are distributed between the particles at the end of simulation time. In Secs. VI & VII, the implications of the symmetries of the system for the emergence of a current are considered. In Sec. VIII, we explore the structure of phase space. In particular, we investigate the invariant sets in the dynamics connected with chaotic saddles. Furthermore, we relate the character of the underlying dynamics, involving almost integrable motion, transient chaos, and permanent chaos, to the different transport scenarios. Finally, we summarize and draw conclusions from our investigation.

II. SYSTEM OF COUPLED PARTICLES

The model used is Hamiltonian and of the form

$$H = \sum_{n=1}^{2} \left[\frac{p_n^2}{2} + U(q_n) \right] + H_{\text{int}}(q_1, q_2), \tag{1}$$

where q_n and p_n $(n = 1,2)$ are the canonically conjugate positions and momenta of coupled particles of unit mass evolving in a spatially symmetric and periodic washboard potential. The potential, of unit period, is given by

$$U(q) = U(q+1) = \frac{1 - \cos(2\pi q)}{2\pi}. \tag{2}$$

The particles are coupled via the interaction term

$$H_{\text{int}}(q_1, q_2) = D \left[1 - \frac{1}{\cosh(q_1 - q_2)} \right], \tag{3}$$

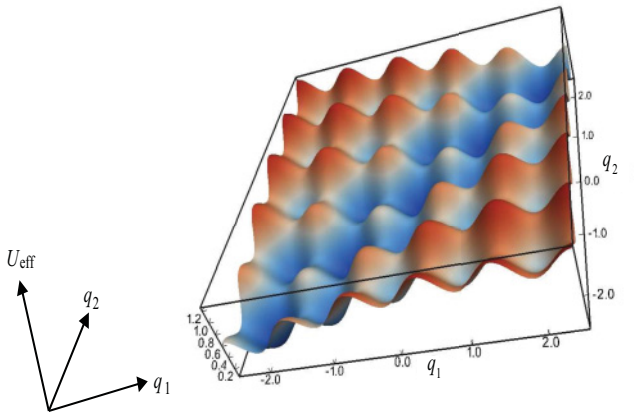

FIG. 1. (Color online) Plot of the effective potential ($D = 0.581\,69$). The main diagonal contains the regions of lowest potential energy.

which is dependent on the distance $d = |q_1 - q_2|$. The strength of this coupling is regulated by the parameter D. It is important to note that asymptotically the gradient $\frac{dH_{\text{int}}(x)}{dx}$ goes to zero, i.e., as the relative distance $|q_1 - q_2|$ increases, the related interaction forces, $\partial H_{\text{int}}/\partial q_1$ and $\partial H_{\text{int}}/\partial q_2$, vanish asymptotically, allowing transient chaos [18–20]. That is, for large distance $|q_1 - q_2| \gg 1$, the interaction vanishes with the result that the two degrees of freedom decouple, rendering the dynamics regular. The effective potential will be defined as

$$U_{\text{eff}}(q_1,q_2) = U(q_1) + U(q_2) + H_{\text{int}}(q_1,q_2). \tag{4}$$

An example of the landscape of the effective potential is shown in Fig. 1 with $-2.5 \leqslant q_1 \leqslant 2.5$ and $-2.5 \leqslant q_2 \leqslant 2.5$. We see energies in the potential ranging from 1.21 (dark orange) to 0 (dark blue). Crucially, along the diagonal (blue area) we have the interaction region, which is where the complexity in the system is manifested.

The equations of motion are given by

$$\ddot{q_1} = -\sin(2\pi q_1) - D\left[\frac{\tanh(q_1 - q_2)}{\cosh(q_1 - q_2)}\right], \tag{5}$$

$$\ddot{q_2} = -\sin(2\pi q_2) + D\left[\frac{\tanh(q_1 - q_2)}{\cosh(q_1 - q_2)}\right]. \tag{6}$$

The initial conditions, $q_2 = p_2 = 0$, for the dynamics are chosen such that (isolated) particle B is situated at the bottom of a well of the washboard potential and hence possesses no energy. Particle A, possessing a sufficient amount of energy to overcome the washboard energy barriers, will be sent from the asymptotic-free region into the region containing particle B and here an energy transfer will take place, the extent of which depends on the coupling strength.

For $D = 0$, we have an uncoupled system. Thus the dynamics of the system will be decided by two integrable subsystems. In effect, this means that the particles initially with energy will hold onto this energy for all time. These particles will pass through the potential landscape unhindered and consequently remain in regular motion. In contrast, the particles that are initially at rest will be unable to gain any energy via an interaction with the other particles and will thus remain at rest for all time.

For $D \neq 0$, the particles can interact via the interaction potential and exchange energy. This exchange will excite the additional (initially resting) particle and, to varying degrees, influence the motion of the particle that has entered the "interaction region." Again, it is important to note that both components of this system are open and thus it is feasible that either particle will escape. For large $|q_1 - q_2| \gg 1$, the interaction between the particles vanishes and again we see the dynamics represented by regular motion, with the possibility of both particles escaping independently excluded (see Sec. VI).

As mentioned earlier, the initial conditions for particle B will be $q_2 = p_2 = 0$. The particle A starts as a virtually free particle in the *asymptotic* region, i.e., it approaches the interaction region from a far distance. The initial amount of energy $E = 0.9$ lies above the highest possible energy of the saddle-center points, but below almost all of the saddle-saddle points of the effective potential (see further in Sec. VI). The initial positions of the particles A are contained within the well whose minimum is located at $q \simeq -25$ and the corresponding initial momenta are determined as those points populating, densely and uniformly, the level curve

$$E = \frac{1}{2}p_1^2 + U(q_1) + H_{\text{int}}(q_1,0), \tag{7}$$

in the (q_1, p_1) plane. Asymptotically, the interaction potential attains a value approaching D. Therefore, as the particles begin in the asymptotic region and as the initial conditions depend explicitly on D, no two sets of initial conditions will be the same. Two examples of these initial conditions are shown in Fig. 2. The energy will be fixed at $E = 0.9$, which is almost three times the barrier height of the washboard potential, $E_b = 1/\pi \approx 0.3183$. It should be emphasized that for particle B to escape, it must gain a sufficient amount of energy from its interaction with particle A. With no interaction, this system will contain a strong positive current, as particle A can escape to infinity feeling no effect from particle B.

There are a number of questions that we will address. First, can particle B gain enough energy to escape from its starting potential well, or is particle B's presence of little or no consequence to the overall dynamics of the system? Second, in the case that particle B does escape, what subsequently happens to both particles? Finally, assuming that particle B's presence is significant, can it influence the dynamics in such a way that there is a reversal of the direction of the current, or even a suppression of the current? These questions will be answered in the subsequent sections.

To partially answer the first and second questions, we will illustrate some of the qualitatively different transport scenarios that are present in this system by varying the strength of the coupling parameter D. Before this, however, we present a table of D values that will be frequently used in this paper along with their respective currents. Particle current is assessed quantitatively by the mean momentum, which is defined by taking the averaged momentum of an ensemble of particles, i.e.,

$$p = \frac{1}{T_s}\int_0^{T_s} dt\langle p(t)\rangle, \tag{8}$$

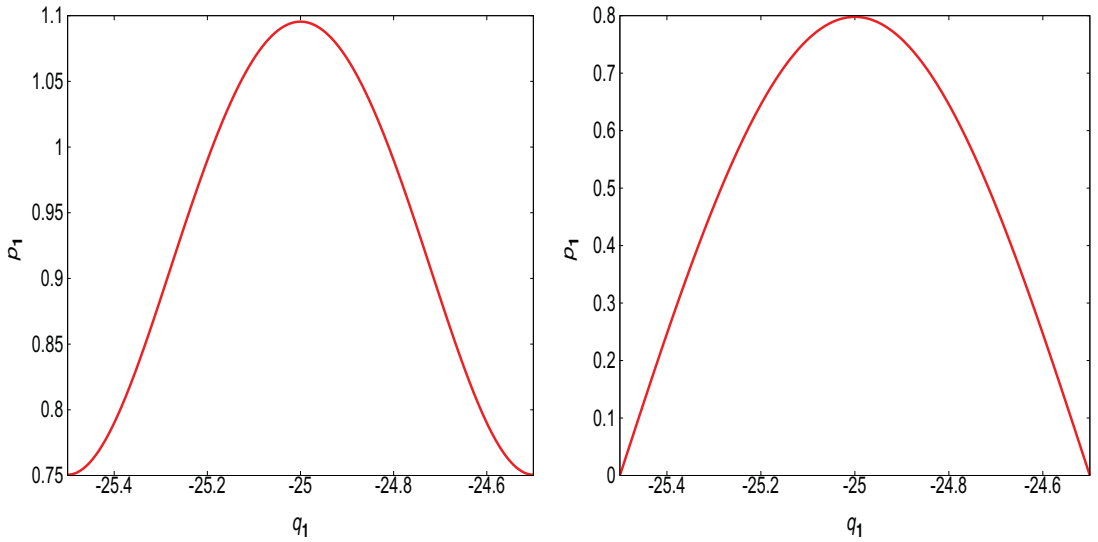

FIG. 2. (Color online) Initial conditions (q_1, p_1) for $D = 0.3$ and $D = 0.581\,69$, respectively.

where T_s is the simulation time, and the ensemble average is given by

$$\langle p(t)\rangle = \frac{1}{N}\sum_{n=1}^{N}\sum_{i=1}^{2} p_{i,n}(t), \tag{9}$$

with N being the number of initial conditions. The current will be discussed in detail in Sec. III:

D	Current
0.3	0.925
0.5613	−0.239
0.5617	0.262
0.5672	0.009
0.58169	−0.0001

Figure 3 contains plots showing the temporal evolution of the coordinates q_1, q_2 for five different D values. For comparison, for each D value, the initial positions of the pair of particles will be the same, i.e., with $q_1(0) = -25.5$ and $q_2(0) = 0$, and the initial momentum of particle A follows from the relation in Eq. (7), while particle B has zero momentum, $p_2(0) = 0$. Slightly altering these initial conditions can have a large impact on the path that the particles will take, as for a large range of the coupling strength the dynamics will be chaotic. In addition, for the same D values, Fig. 4 illustrates the time evolution of the partial energies which are defined as

$$E_1 = \tfrac{1}{2}p_1^2 + U(q_1) + \tfrac{1}{2}H_{\rm int}(q_1,q_2), \tag{10}$$

$$E_2 = \tfrac{1}{2}p_2^2 + U(q_2) + \tfrac{1}{2}H_{\rm int}(q_1,q_2), \tag{11}$$

with E_1 and E_2 being the partial energies of particles A and B, respectively, and with the interaction energy being divided evenly between the particles. From conservation of energy, the quantity $E = E_1 + E_2$ remains constant. It is important to note that as D increases so does the initial amount of energy held in the interaction potential, therefore giving less portion of the total energy to the first two terms of the energy of particle A in Eq. (10).

With $D = 0.3$ [Figs. 3(a) and 4(a)], we see that particle A is able to pass straight through the interaction region almost unscathed. Particle B does receive some energy from the interaction, but this energy only allows for small oscillations about its starting position. This setup favors a strong, positive current. With regard to particle B leaving its initial potential well, there appears a blowup at $D \approx 0.562$, after which we can expect both particles to travel multiple potential wells together. As can be seen in Figs. 3(b) and 3(c), both with $D < 0.562$, particle B can largely influence the path of particle A without actually leaving its starting potential well. Setting D to 0.5613 [Figs. 3(b) and 4(b)], we see that the dynamics of the system is quite different. The interaction between the particles is such that particle A can pass through the interaction region (to a certain extent) and subsequently be pulled back, escaping in the negative q direction and thus contributing to current reversal. Again particle B receives little energy from the interaction, as can be seen in Fig. 4(b). A similar phenomenon can be seen for $D = 0.5617$ [Figs. 3(c) and 4(c)]. This time particle A oscillates around $q = 0$ a number of times before escaping in the positive q direction maintaining the original direction of the current. Some of the most interesting behavior observed in this system can be seen in the remaining two figures. Figures 3(d) and 4(d) show a trajectory with $D = 0.5672$. There are a number of striking things that can be noted about this trajectory. First, the duration of time that the trajectories "stick" together before one escapes. In this case, particle B escapes in the positive q direction. This is substantially longer than the escape times presented in the previous figures. Also, both particles take excursions to the left and right before the escape of particle B. However, the most notable thing about this figure is that it is particle B that escapes, not particle A as for the previous D values. Thus particle B is able to gain enough energy to escape from its starting potential well, and subsequently from any force that it feels from particle A. Particle A has sacrificed its energy and has become trapped. This situation describes an interchange of the roles played by particles, with the initially free particle

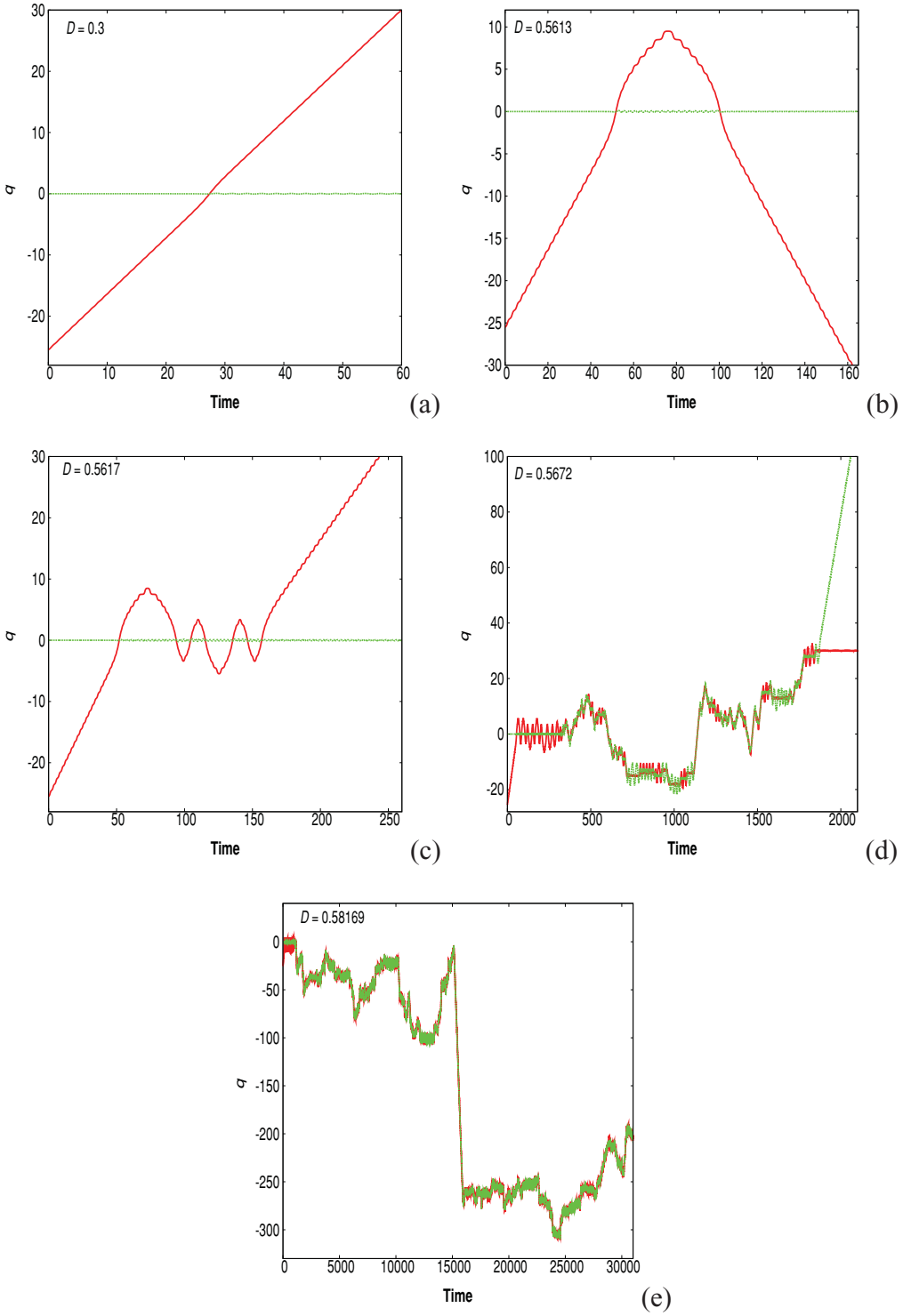

FIG. 3. (Color online) Example trajectories using a range of different D values. The red (solid) line shows the temporal evolution of particle A, while the green (dashed) line shows the time evolution of particle B. The initial conditions for each trajectory are chosen as $q_1(0) = -25.5$ and $q_2(0) = 0$.

becoming trapped and the initially trapped particle becoming free. The final figures [Figs. 3(e) and 4(e)], with $D = 0.561\,69$, show similar behavior in that the particles seem to "stick" together. However, neither particle escapes, but instead are, in some sense, stuck to each other for the duration of the simulation. This is a process known as dimerization, where the particles, each acting as a monomer, form a bound unit. This process is evident in some of the previous figures; however, in this case, the process is permanent. Both particles undergo large excursions along the line $q_1 = q_2$. It can be seen in Fig. 4(e) that, for this particular D value, the particles are in a continual and, most importantly, substantial energy exchange.

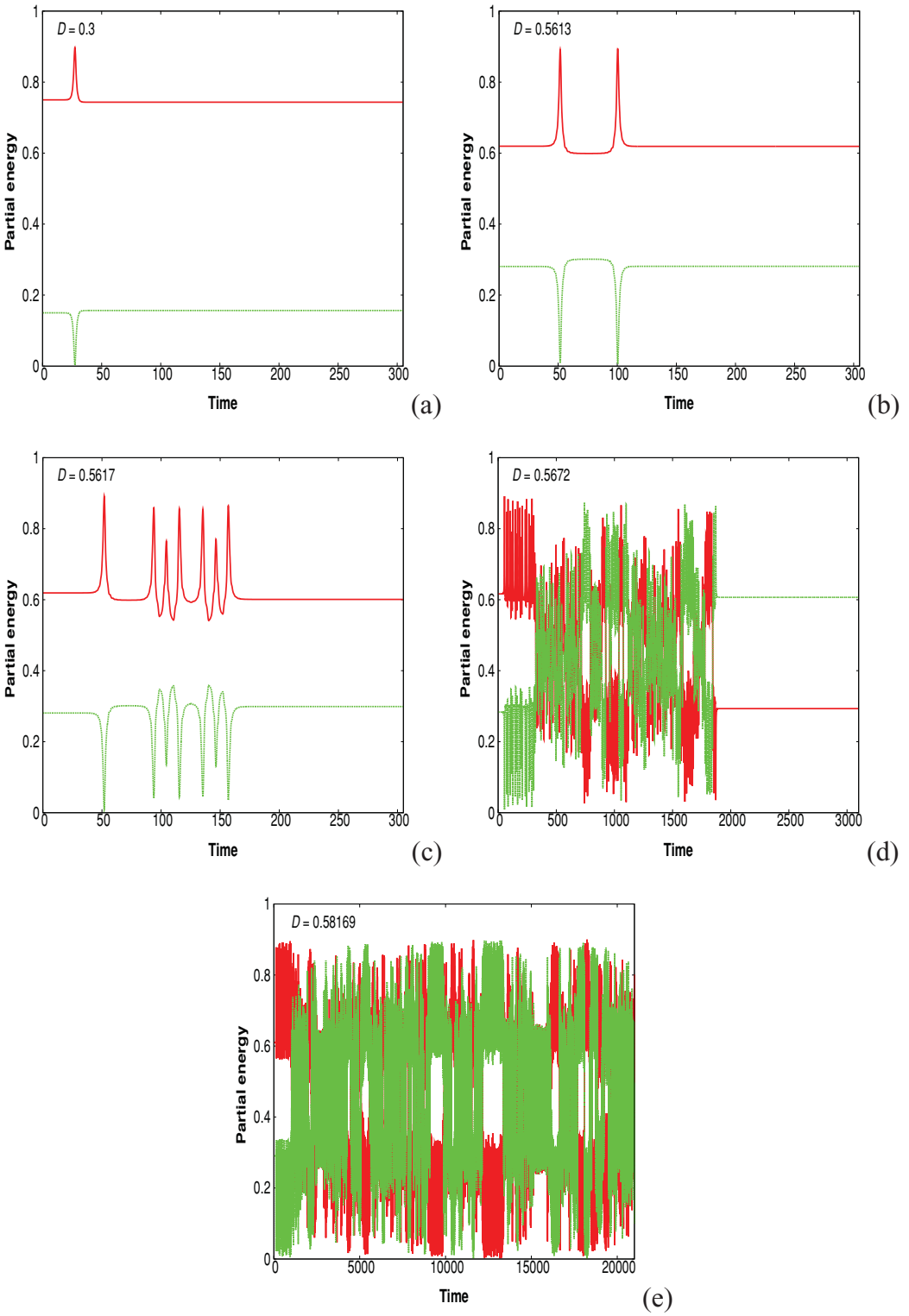

FIG. 4. (Color online) Partial energies corresponding to the trajectories in Fig. 3. Again, the temporal evolution of particle A is shown by the red (solid) line and particle B by the green (dashed) line.

This allows the particles to travel together in an erratic fashion undergoing multiple changes of direction and visiting multiple potential wells.

A characteristic of each figure is that when particle A enters the interaction region there is a slight increase in its momentum. This acceleration is due to the dip in the potential landscape created by the interaction potential. Particle A thus usurps some of the energy contained in the interaction potential. Importantly, the escape of one particle at the expense of the other, and therefore an increase in the distance between

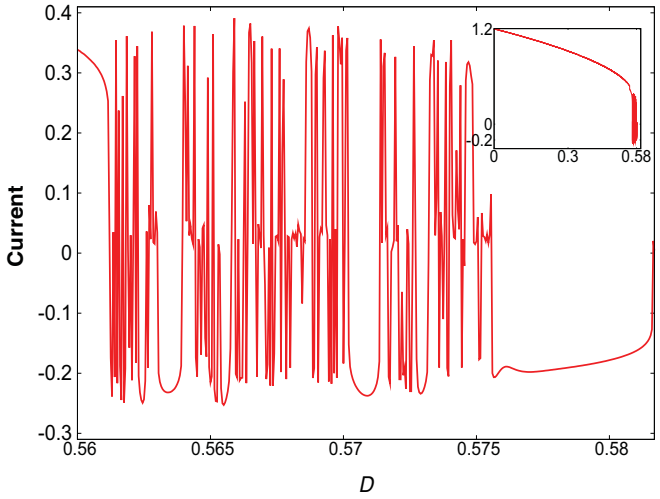

FIG. 5. (Color online) Current as a function of D. The inset displays the current for the full range of D values, namely $0 \leqslant D \lesssim 0.5817$. The main figure displays, in detail, the sensitivity of the current to changes in D. This corresponds to the bottom right corner of the inset.

the particles, restores the initial amount of energy contained in the interaction potential.

III. PARTICLE CURRENT

We now consider the current induced by directed particle transport. Figure 5 shows the current, as defined in Eq. (8), for the system as a function of D. Strikingly, one notices that there are intervals for which the current is very sensitively dependent on D. Small changes to this parameter result in drastic changes to both the magnitude and direction of the current. (In fact, if we choose an even finer step size for D, we find that it is even more sensitive.)

For small D values, we see a strong positive current. This is because particles feel little-to-no effect when entering the interaction region and pass straight through relatively unscathed. As D increases, there is a gradual decrease in the current until $D \approx 0.561$, where there is a sharp decline in the current (see inset of Fig. 5). After this D value, the magnitude and direction of the current oscillates erratically until $D \approx 0.5756$. That is, as the coupling parameter D is varied, the current, originally in one direction, can drop to zero and then reverse. In the forthcoming, we associate the frequent current reversals to the underlying transient chaotic dynamics. For $D \gtrsim 0.5756$, the current plateaus and finally at $D \approx 0.58$ the current makes a sharp rise, becoming positive, before tending to zero. This sharp rise can be understood if we look at the interaction potential. As mentioned in Sec. II, for the initial dynamics, as D increases so does the energy contained in the interaction potential and consequently particle A has less energy. More concretely, as $D \to (0.9\text{–}1/\pi \approx 0.5817)$, then $E_A \to 1/\pi \approx 0.3142$ (barrier height of the washboard potential). Therefore, particle A will have sufficient energy to make it over the potential barriers it passes while traveling to the interaction region, but once there will not be able to pass through and must interact with particle B.

Another interesting feature of this plot is the numerous plateaus that appear for negative values of the current. This indicates that there are certain ranges of D where the current does not oscillate erratically, but rather stays almost constant.

IV. PARTICLES SOJOURN IN INTERACTION REGION

A more direct way of examining the effect that the coupling strength has on the particles is to calculate the amount of time that particles A and B spend in the interaction region. More formally, we have calculated the time that the particles satisfy the condition

$$|q_1(t) - q_2(t)| \leqslant 10, \tag{12}$$

outside of which the gradient of the potential will almost be equal to zero.

Figure 6 (left panel) shows the sojourn times for an ensemble of initial conditions corresponding to $D = 0.5617$ and $D = 0.5672$ as a function of the angle $\alpha = \tan^{-1}[p_1(0)/q_1(0)]$, which can be viewed as the incident angle in the (q_1, p_1) phase plane of the initially free particle A. We see with the lower D value that the particles all spend a relatively short time in the interaction region and that the time corresponding to each initial condition is almost the same. Associated with this is a fairly large current, $\bar{p} = 0.262$, indicating that the particles leave the interaction region in a preferred direction. In contrast, for the second D value, the time for each initial condition is noticeably longer than in the previous case. Further, these times are much more varied and there is a large difference between the smallest and greatest time for this ensemble (approximately 2700 time units). That is, as a hallmark of chaotic scattering [21–25]; the sojourn time depends sensitively on changes of the initial values because chaotic saddles, formed by the intersecting stable and unstable manifolds of unstable periodic orbits, govern the dynamics. In more detail, escaping trajectories follow the unstable manifolds of saddle points, whereas there are trajectories that remain in the interaction region or spend at least some time there before they escape as a consequence of the presence of chaotic saddles. From the corresponding small value of the current, $\bar{p} = 0.009$, we infer that the exit of the particles from the interaction region proceeds such that they virtually balance each others' contribution to the net current. The window containing no points is due to the fact that with a lower D value the range of momenta taken initially by an ensemble of particles A is smaller than the range for a larger D value. This is clearly seen in the example initial conditions shown in Fig. 2.

Finally, in the case that $D = 0.581\,69$ (Fig. 6, right panel), corresponding to a vanishingly small current, we see all of the particles spend the entire duration of the simulation in the interaction region (50 000 time units). This is a possible mechanism that allows for the reduced current that can be seen.

V. ENERGY REDISTRIBUTION PROCESSES

In order to gain more insight into the dynamics of the system, a statistical analysis, going beyond the consideration of individual trajectories (cf. Sec. II), is carried out. Previously, we have looked at the partial energies for particles A and

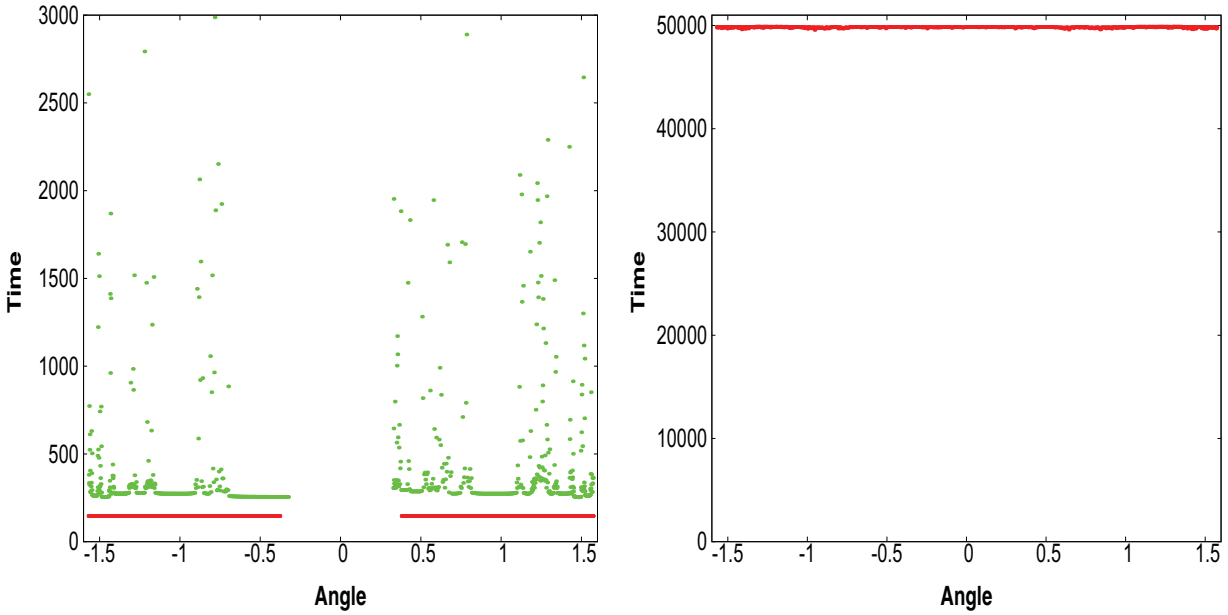

FIG. 6. (Color online) Sojourn time of an ensemble of particles in the interaction region. Left: The green (scattered) points show the time for the ensemble when $D = 0.5617$. Similarly, red (lower line) is for the particles when $D = 0.5672$. Right: Same as left with $D = 0.581\,69$.

B for the duration of a simulation using individual initial conditions (discussed in Sec. II). Now we will make use of histograms displaying the distribution of particle energies, using an ensemble of $N = 10^3$ initial conditions, at the end of the simulation time $T_s = 10^5$. For continuity, we will examine the histograms corresponding to the five D values used in earlier sections.

In Fig. 7(a) ($D = 0.3$), we see that at the end of the simulation it is particle A, for the entire ensemble, that possesses the majority of the energy in the system. While particle B does possess some energy, it is not sufficient for it to escape from its starting potential well. Since the energy of particle B is below the energy of the confining center-saddle points, escape of particle B over the barriers is prevented. A more detailed consideration of the potential landscape will be presented in the next section.

We see a similar histogram in Fig. 7(b) ($D = 0.5613$). The difference this time is that particle A has sacrificed some of its energy to particle B. This is not unexpected if we consider the example trajectory shown in Fig. 3(b)—the interaction with particle B has a significant impact on the trajectory of particle A.

Again in Fig. 7(c) (with $D = 0.5617$), we have a similar histogram as seen in Figs. 7(a) and 7(b) with a further loss in energy for particle A, and a gain for particle B, and thus the final particle energies lie closer together. A slightly more intriguing histogram is presented in Fig. 7(d) ($D = 0.5672$). This D value corresponds to that of Fig. 3(d), where it is particle B not particle A that escapes. Consequently, the histogram shows that, indeed, there are some particles B that possess the majority of the energy at the end of the simulation. However, it is clear that, for the ensemble, the majority of particles that contain most of the energy are, in fact, particle A.

Finally, in Fig. 7(e) ($D = 0.581\,69$), we see that there is a large distribution in the final energies of each particle, with no obvious bias favoring the partial energy of any particle.

These histograms for the various D values do not give a full indication of what the current will be for those respective D values. They do, however, allow us to make assumptions. For example, Fig. 7(a) shows that particles A contain almost all of the energy at the end of the simulation. We therefore expect that particle A, for the entire ensemble, will make a large contribution to the net current. Further, if we were naively to include the corresponding example in our assumption, we might conclude that there will be a large positive net current for the ensemble.

If we were to look at the next D value and make similar assumptions, we would conclude that again there is a large positive net current. This time, however, the current would not be quite as strong, as the final energies for the ensemble indicate that particle A has less energy.

Now, if we were to take the final D value, we might conclude that, because of the spread of energies for both particles, the current will be quite small.

Importantly though, nothing definite can be said about the current for an ensemble of particles until a further investigation of the phase-space structure has been carried out. This we do now.

VI. MANIFOLDS AND SADDLE POINTS

A more global understanding of the dynamics in phase space has been obtained by examining the equilibria of the system and tracing the manifolds of unstable periodic orbits. The intricate network of intersecting invariant manifolds associated with the numerous unstable equilibria of the two-dimensional potential landscape, U_{eff}, contributes to

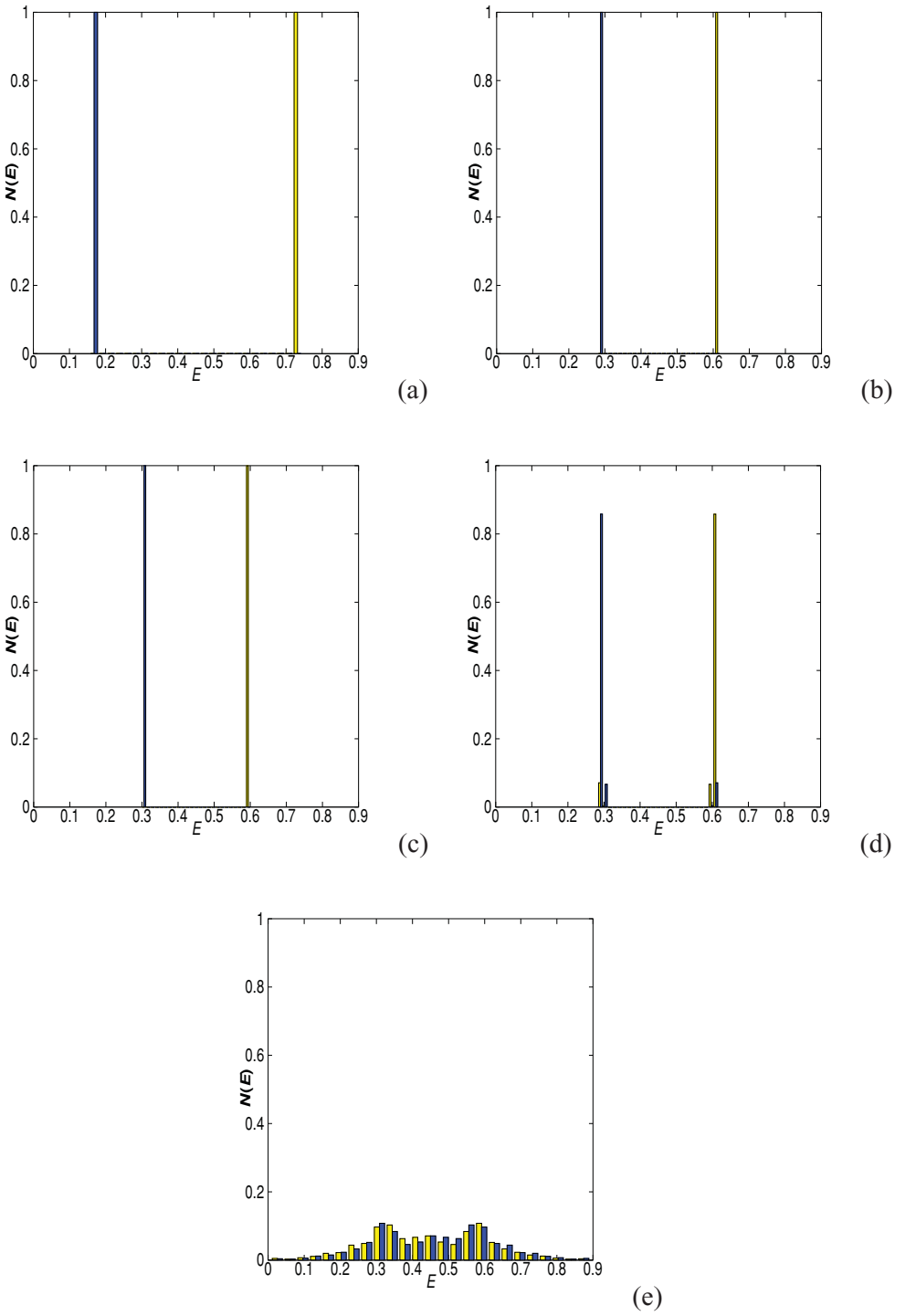

FIG. 7. (Color online) Histograms displaying the final partial energies, again using the five D values from the table in Sec. II, of particles A [blue (dark gray)] and B [yellow (light gray)] for an ensemble of initial conditions.

rather complicated dynamics. By way of example, for an illustration, the unstable invariant manifolds of a saddle-type periodic orbit associated with the saddle-center point located at $q_1 = -12.5$ and $q_2 = 0$ are displayed for two different D values to highlight or reinforce some of the complex behavior discussed in previous sections. In particular, we calculate a point distribution on the relevant stable or unstable manifold branches of the saddle-type periodic orbit. These are calculated by numerically integrating from an initially equidistributed point set. To ensure accuracy is maintained, the value of the energy is monitored over the integration time frame. Our aim here is to show, for these D values, some of the various channels that a particle can take that will result in current reversals and current suppression.

The left panel in Fig. 8 shows the scattering nature of this system. We see that, with $D = 0.5617$, channels along the unstable manifold exist for both coordinates, q_1 and q_2, in the positive and negative directions (inset in left panel). However,

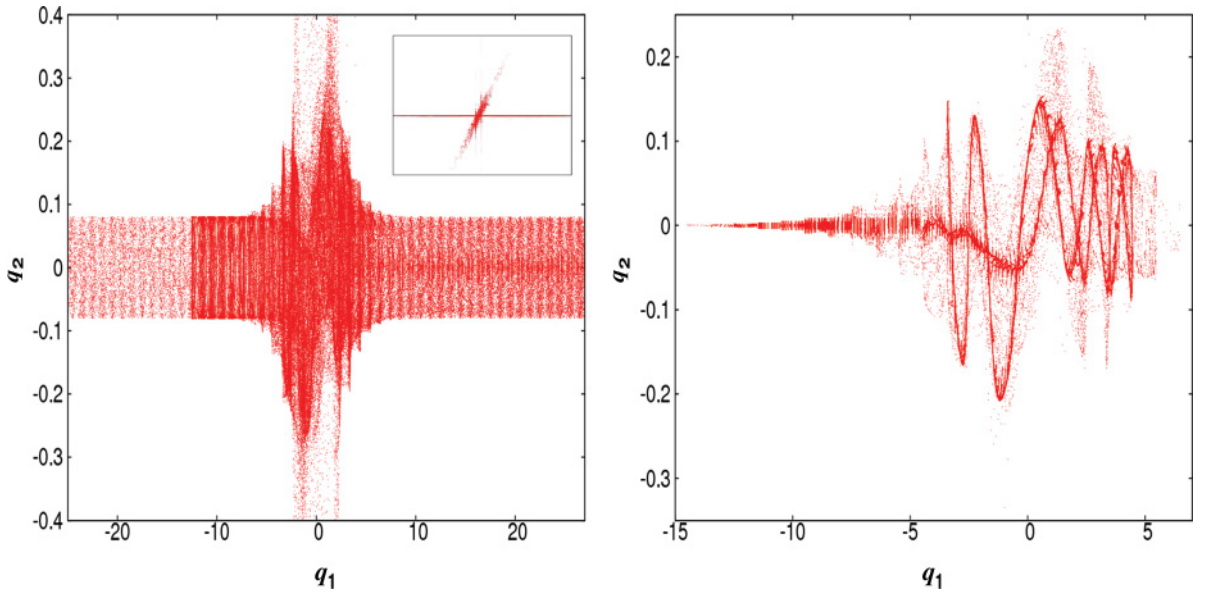

FIG. 8. (Color online) Manifolds for $D = 0.5617$ and $D = 0.581\,69$. The inset shows the manifold extended in configuration space.

it is clear that the favored channel takes the particles in the positive q_1 direction where, subsequent to the period of transient chaos, it becomes asymptotically free by settling on regular motion. This is in direct agreement with the current value produced using this D value. The right panel in Fig. 8 illustrates partially how a vanishingly small current has emerged from the system when $D = 0.581\,69$. The dynamics shows that, provided the corresponding trajectory follows the invariant manifolds of the chaotic saddle, particle A (respectively B) is locked in paths provided by the unstable manifold that will see it undergo many crossings of the line $q_1 = 0$ (respectively $q_2 = 0$), and thus many changes of direction. Subsequently, the contribution to the net current by particle A and particle B, while the particles are locked in such a path, will on average be zero. However, as the example trajectories show, the particles can wander in much wider regions of configuration space as the corresponding trajectory is captured in the intricate network of the chaotic invariant sets consisting of homoclinic and heteroclinic tangles. Nonetheless, due to the symmetric extension of the chaotic invariant set, no preferred direction for the trajectories exists.

As Fig. 5 has shown, the dynamics of the system are sensitively dependent on the strength of the coupling. For a low D value, particle A can pass through the interaction region unscathed. With increasing D, particle A can no longer find a direct route through the interaction region. Instead, it enters into an energy exchange with particle B with both particles trying to find a path out of the interaction region. As, previously discussed, there are numerous possible scenarios for particles A and B, once particle A has reached the interaction region. An explanation for these scenarios comes from the saddle-point energies corresponding to the various D values.

In Fig. 9, some of the locations of the equilibria of the system (for $D = 0.581\,69$), in the range $-10 \leqslant q_1 \leqslant 10$ and $-0.7 \leqslant q_2 \leqslant 0.7$, are shown in the (q_1,q_2) plane. Let (q_{1_i},q_{2_j}) denote the equilibrium point with $q_{1_i} \simeq i/2$ and $q_{2_j} \simeq j/2$. The distortion in configuration space is clear to see. Notably, there is a lack of $q_1 \mapsto -q_1$ and $q_2 \mapsto -q_2$ reflection symmetry. It is this distortion that allows particle B to become excited and potentially leave its starting potential well. The reason being that, with the path of least resistance no longer being along the line $q_2 = 0$, particle A deviates from its hitherto straight line path and thus stimulates particle B.

Figure 10 shows saddle-point energies as a function of D. The left panel, corresponding to the saddle points $(0,2i + 1)$, shows that all of these saddle points are energetically accessible for every D value. In contrast, many of the saddle points $(1,2i + 1)$ (right panel) become energetically inaccessible after a relatively small D value ($D \approx 0.3$). This suggests that these inaccessible saddles form the boundaries of channels

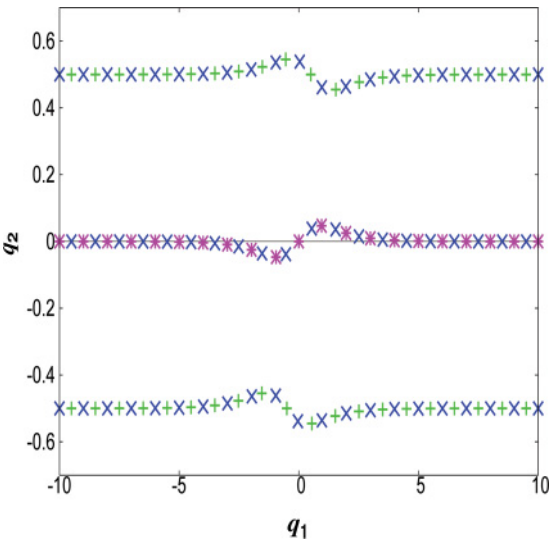

FIG. 9. (Color online) Locations of the (i,j)th equilibrium point in configuration space for $-20 \leqslant i \leqslant 20$ and $-1 \leqslant j \leqslant 1$, for $D = 0.581\,69$. Center-center points are indicated by a star, saddle-center points by a cross, and saddle-saddle points by a plus sign.

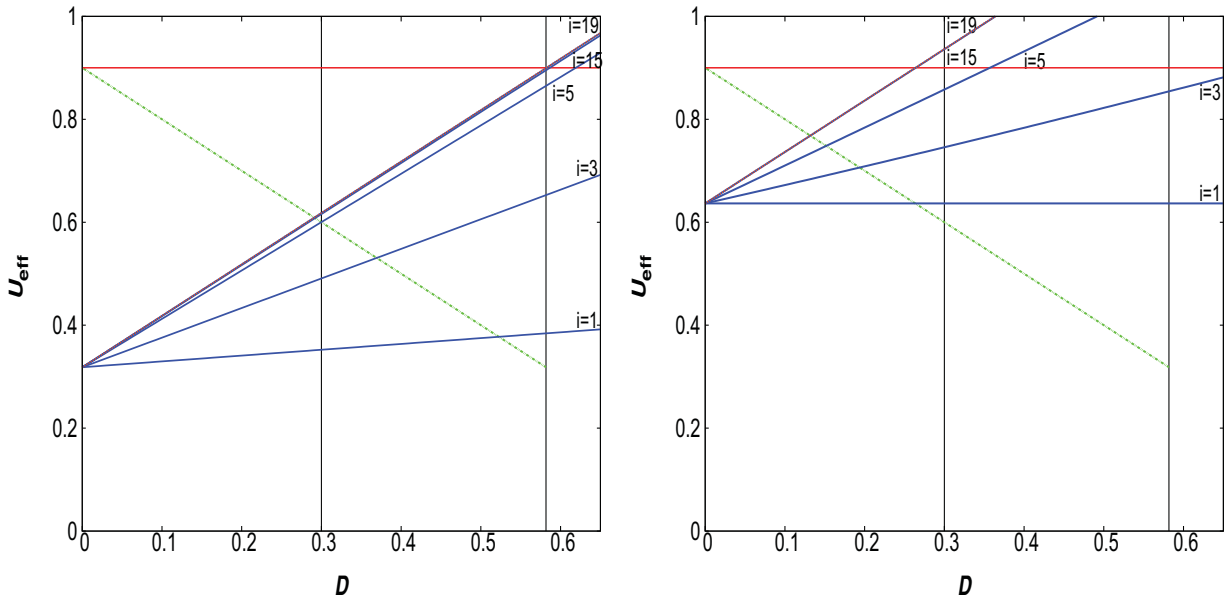

FIG. 10. (Color online) Effective potential as a function of D shown at the saddle points $x_{(0,2i+1)}$ (left panel) and $x_{(1,2i+1)}$ (right panel). The horizontal line indicates the total simulation energy, i.e., $E = 0.9$. The two vertical lines located at $D = 0.3$ and $D = 0.581\,69$ were used in the simulations. The green line (negative slope) shows the initial energy of particle A as a function of D.

guiding the particles. Crucially, even though the paths may be blocked at many points, there are still multiple routes for the particles to wander and thus the possibility of a directed current being produced is not excluded.

Another interesting observation that can be made from these figures is that above $D \approx 0.12$ the saddle energies create barriers that, with the simulation energy $E = 0.9$, only one particle can pass over. In particular, some of the saddle energies attain values greater than 4.5, which eliminates the possibility of both particles undergoing independent escapes. Below $D \approx 0.12$, it is energetically feasible that both particles can have enough energy to mount independent escapes. However, the low coupling strength excludes the possibility of particle B attaining enough energy from the interaction with particle A. Therefore, if one particle escapes, it will be at the expense of the other, which must remain trapped for the entire simulation.

The green lines (negative slope) superimposed on both plots in Fig. 10 going from the points (0.0,0.9) to $(0.5817, 1/\pi)$ show the initial energy of particle A as a function of D. In the left plot, we see that for $D \lesssim 0.28$ particle A will initially possess enough energy to overcome all of these barriers. Increasing D beyond this value will mean that, for particle A to escape, it will need additional energy, which has to come from the interaction potential. When D is sufficiently large, particle A will have insufficient energy to overcome any of the potential barriers. This means that a significant interaction will ensue and that particle B's role in the dynamics will be fundamental. A similar situation unfolds in the right-hand plot. However, many of the saddle points become energetically inaccessible for increasing D, meaning that the particles will be unable to obtain enough energy from the interaction potential to overcome these barriers.

The scenario with a vanishingly small current (i.e., $D = 0.581\,69$) still requires an explanation. Examining the saddle-point energies at this D value (shown by a vertical line in the plots), we see that almost all of the saddle points $(1,2i+1)$ are energetically inaccessible. Only those saddle points (1,1) and (1,3) can be overcome. As already noted, all of the saddle points $(0,2i+1)$ are energetically accessible. However, those saddle points with $i > 4$ have energies that tend to 0.9. Thus for a particle to pass over these barriers requires that the particle holds all energy contained in the system. The strength of the coupling almost certainly precludes such a situation and therefore both particles are forced to wander chaotically in the interaction region. Importantly, as D increases, so does the size of the energetically inaccessible regions. With increasing D, these regions join, forming an impenetrable barrier that the particles cannot pass, and thus leaving them to wander in the interaction region. This is depicted in Fig. 11.

VII. SYMMETRIES CONSIDERATIONS

To gain more insight into the occurrence of the different transport scenarios, it is illustrative to consider the symmetries present in the system. First, the washboard potentials, $U(x)$, are each periodic (of period 1) in their respective arguments and, in addition, they are invariant under reflections in their arguments:

$$U(x) = U(-x). \tag{13}$$

Also, the interaction potential, $H_{\text{int}}(q_1,q_2)$, is invariant with respect to changes in the sign of its argument, i.e.,

$$H_{\text{int}}(q_1,q_2) = H_{\text{int}}(-q_1,-q_2). \tag{14}$$

Notice that with the inclusion of H_{int} the effective potential $U_{\text{eff}} = U(q_1) + U(q_2) + H_{\text{int}}(q_1,q_2)$ is not periodic. Most importantly, the system exhibits the particle exchange symmetry $(p_1,q_1) \longleftrightarrow (p_2,q_2)$. Apart from these spatial symmetries, the Hamiltonian is even in the momenta $p_{1,2}$ establishing

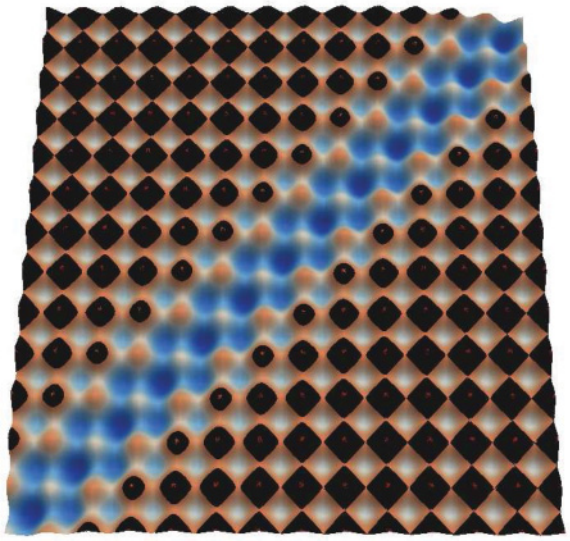

FIG. 11. (Color online) Shown for $D = 0.581\,69$ is the effective potential. The energetically inaccessible regions are shown in black.

time-reversible symmetry of the system. As a consequence, for a set of uniformly distributed initial conditions populating the entire energy surface, the current will be zero. However, the energy surface is unbounded along the coordinates and thus cannot in practice be populated with a finite set of initial conditions. In fact, for our scattering problem, when one of the particles is sent from a certain finite range of positions $-\infty < q_l \leqslant q_1(0) \leqslant q_r < 0$ in the asymptotically free region toward the other particle with $p_2(0) = q_2(0) = 0$, the corresponding sets of initial coordinates $[q_1(0),q_2(0)]$ are finite and spatially localized. Moreover, as the incoming free particles are sent in from one side only they have momentum of definite sign, $p_1(0) > 0$, so that a current exists at least as long as the incoming (traveling) particle has not yet reached the interaction region. From the above symmetry considerations, it follows that the Hamiltonian is inversion symmetric with regard to the momenta and coordinates, i.e., $H(p_1,p_2,q_1,q_2) = H(-p_1, -p_2, -q_1, -q_2)$. However, inversion symmetry is not reflected in our choice of localized initial conditions. Crucially, in the absence of the corresponding counterpropagating particles emanating from initial conditions $[-q_1(0),q_2(0) = 0]$ and $[-p_1(0),p_2(0) = 0]$, the inversion symmetry is broken. It depends then on the interaction process between the two particles [the scattering process in the landscape of the effective potential $U_{\text{eff}}(q_1,q_2)$] whether the current is preserved or reversed or even suppressed. In the context of current suppression, it is illustrative to recall Curie's principle, which states that if a phenomenon is not prohibited by a specific symmetry, then in general the phenomenon will occur [26,27], which, in other words, rules out the presence of accidental symmetries. Nevertheless, in our system, accidental symmetries [26,27], reflected in a vanishing current, occur as a result of fine-tuning of the coupling strength parameter (cf. Fig. 5). It should be stressed that upon arbitrarily slight tuning of the coupling strength parameter away from the position of a vanishing current a nonzero current results, that is the accidental symmetry is destroyed, which is the hallmark of structural instability.

VIII. PHASE-SPACE DYNAMICS

In Sec. II, we illustrated some qualitatively different transport scenarios that are present in the system. As a further illustration of the phase-space dynamics, we present here a method that illuminates the dynamics of each particle, using various values of D. Trajectories, evolving in the four-dimensional phase space on the three-dimensional energy hypersurface, can be represented by examining the following surfaces:

$$\Sigma_1 = \{q_1, p_1 | U(q_2) = 0\}, \tag{15}$$

and

$$\Sigma_2 = \{q_2, p_2 | U(q_1) = 0\}, \tag{16}$$

where the surface of section Σ_1 will show the dynamics of particle A and Σ_2 that of particle B, respectively. Note that, for both surfaces, the coordinates q_1 and q_2 are shown mod(1). It should be noted that the dimension of the phase space is four and thus Arnold diffusion is possible. However, Arnold diffusion will only happen on time scales much larger than those relevant for particle transport [28] and therefore we do not consider it further.

Figure 12 shows the surfaces of section for $D = 0.3$, $D = 0.5672$, and $D = 0.581\,69$ (from top to bottom with increasing size of D and Σ_1 on the left and Σ_2 on the right). We see that for a fairly low value, $D = 0.3$, exclusively regular motion occurs. Importantly, particle A always maintains a strong positive momentum characterized by the densely covered curves associated with rotational motion, while particle B's motion is bounded with it undergoing small oscillations about its starting position. With this D value, particle B contributes nothing to the net current. However, with the significant contribution from particles A, with all trajectories evolving in the range of positive velocities, we can expect a strong positive current. Increasing the coupling strength to $D = 0.5672$, we see much more interesting and complex behavior in phase space. In particular, many of the particles initially at rest escape from their starting potential well. This escape happens after a chaotic transient, which sees particle B gaining enough energy to escape. On the surfaces Σ_1 and Σ_2, this motion is characterized by scattered points (representing the chaotic transient) and densely covered curves (representing the rotational motion that ensues after a particle has escaped). Furthermore, as there is only sufficient energy for one particle to escape, the remaining particle becomes trapped and oscillates around the bottom of a potential well. This can be seen on the surfaces as the area occupying the center of these figures.

There do, however, remain particles that stay trapped in this potential well. Zooming in on the central region of this figure reveals that there is indeed regular dynamics present in the system. In addition, there is also chaotic motion for some of the particles. This corresponds to the chaotic transient that the particles experience before one escapes. Furthermore, as was seen in Sec. II, it is possible for particle B to escape. This is reinforced by Fig. 3(d). Finally, for a strong coupling $D = 0.581\,69$, both surfaces are largely covered by scattered points (bottom panels). This indicates that the motion of the particles is highly chaotic. There does appear to be some

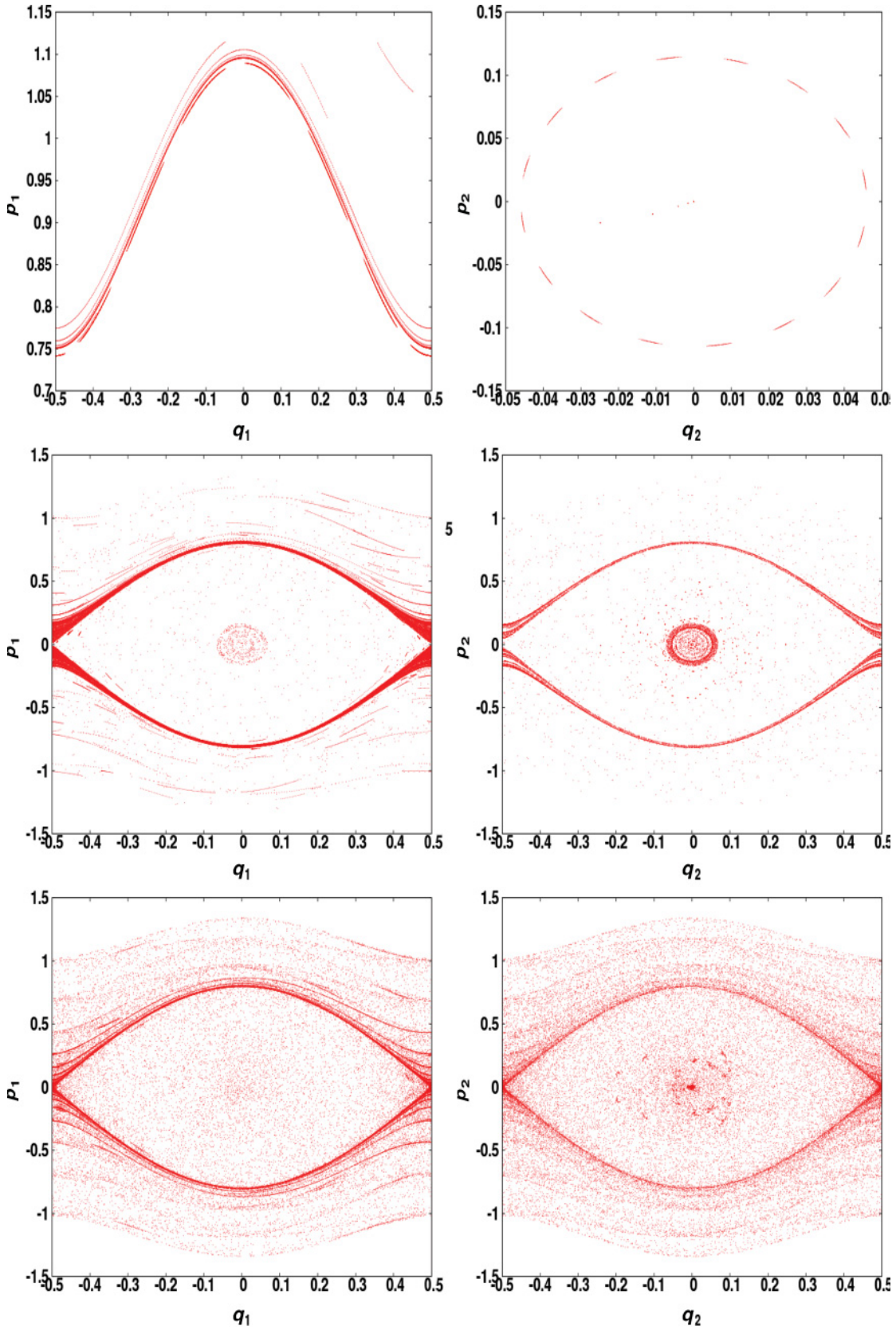

FIG. 12. (Color online) Surfaces displaying the phase-space dynamics of particle A (panels on the left) and particle B (panels on the right) for three different D values. From top to bottom, these are $D = 0.3$, $D = 0.5672$, and $D = 0.581\,69$. The coordinates q_2 and q_2 are presented mod(1).

transport in the dynamics, but this has two explanations. First, the motion is initially regular with particle A being free. Secondly, as was seen in Fig. 3(e), both particles can travel large distances in a relatively short time, in interludes of rotational motion, but afterward become once again trapped in potential wells for some time. However, the particles do return to full chaotic motion after this transient of almost regular motion. Furthermore, with respect to the lines $p_1 = 0$ and $p_2 = 0$, the surfaces appear to be symmetric. This indicates that an ensemble of particles contribute nothing to the net current.

IX. RESULTS AND CONCLUSION

We have studied the Hamiltonian dynamics of particles evolving in symmetric and periodic washboard potentials. A free particle A is sent into a region containing particle B, which is at rest, where they interact. This interaction is local in that, if the distance between the particles is large, then neither particle's motion will be affected by the other. Some of the numerous qualitatively different transport scenarios present in this system have been demonstrated, together with the corresponding energy transfer that takes place between the two particles. The most interesting of these scenarios is that in which it is particle B, not particle A, that escapes. The figure containing the partial energies of the particles clearly shows the chaotic exchange of energy that results in particle A sacrificing its energy and allowing particle B to escape. This scenario is particularly interesting as both particles' momentum contributes to the net current.

More general observations on the type motion have been made. Initially, the motion of the system is regular. Once the particles are sufficiently close, there exists chaotic motion with the parameter D deciding the nature of this chaos. Either it will be a transient, with one or the other of the particles escaping, or it will be permanent, with the particles being locked together forever. This result is interesting, as it shows that there exist open channels, where the particles scatter off each other in the potential landscape, and closed channels, where the particles form a bond, i.e., a dimer. The duration of the transient of chaos is also dependent on the coupling strength, for some values being extremely short and for others being relatively long.

Particular attention has been given to the particle current, notably current reversals and current suppression, and how this is affected by changes in the coupling strength. The sensitive dependence of a current on this coupling parameter is extremely pronounced, with small changes in this strength reversing the direction of the current. In this sense, the coupling strength acts as a switch that when flipped changes the direction of the current. Most astonishing is the fact that it is possible to suppress the current for certain values of this coupling parameter.

In summary, we have demonstrated that it is possible for a system with a strong positive current to undergo multiple current reversals and even current suppression, without the need for external driving or damping, just by varying the coupling parameter.

Finally, as forthcoming investigations are concerned, we point to the corresponding quantum-mechanical scattering problem. In particular, in the context of molecular physics as well as cold-atom physics, the influence of quantum effects on the formation of n-body bound states related with the distinct scenarios of regular motion, on the one hand, and transient and permanent chaos in the potential landscape, on the other, needs to be explored. Furthermore, for the formation of n-mers out of more than two isolated monomers, the key question is whether the interaction between the particles, taking place in a high-dimensional phase space, proceeds such that the energy distribution among them leads to closed channels, i.e., bond formation, as in the way described in this paper for the dimer case.

[1] J. B. Majer *et al.*, Phys. Rev. Lett. **90**, 056802 (2003).
[2] R. D. Austumian and P. H. Hänggi, Phys. Today **55**, 33 (2002).
[3] P. H. Hänggi and F. Marchesoni, Rev. Mod. Phys. **81**, 387 (2009).
[4] S. Flach, O. Yevtushenko, and Y. Zolotaryuk, Phys. Rev. Lett. **84**, 2358 (2000).
[5] S. Denisov, S. Flach, A. A. Ovchinnikov, O. Yevtushenko, and Y. Zolotaryuk, Phys. Rev. E **66**, 041104 (2002).
[6] S. Denisov and S. Flach, Phys. Rev. E **64**, 056236 (2001); S. Denisov, J. Klafter, M. Urbakh, and S. Flach, Physica D **170**, 131 (2002); S. Denisov, J. Klafter, and M. Urbakh, Phys. Rev. E **66**, 046217 (2002).
[7] H. Schanz, T. Dittrich, and R. Ketzmerick, Phys. Rev. E **71**, 026228 (2005).
[8] H. Schanz, M.-F. Otto, R. Ketzmerick, and T. Dittrich, Phys. Rev. Lett. **87**, 070601 (2001).
[9] W. Acevedo and T. Dittrich, Prog. Theor. Phys. Suppl. **150**, 313 (2003).
[10] H. Schanz and M. Prusty, J. Phys. A: Math. Gen. **38**, 10085 (2005).
[11] M. Horvat and T. Prosen, J. Phys. A: Math. Gen. **37**, 3133 (2004).
[12] D. Hennig, A. D. Burbanks, A. H. Osbaldestin, and C. Mulhern, J. Phys. A: Math. Theor. **43**, 345101 (2010).
[13] D. Hennig, A. D. Burbanks, C. Mulhern, and A. H. Osbaldestin, Phys. Rev. E **82**, 026210 (2010).
[14] D. Hennig, A. D. Burbanks, and A. H. Osbaldestin, Physica D **238**, 2273 (2009).
[15] J. L. Mateos, Phys. Rev. Lett. **84**, 258 (2000).
[16] J. L. Mateos, Physica A **325**, 92 (2003).
[17] R. Salgado García, G. Martínez-Mekler, and M. Alanda, Phys. Rev. E **78**, 011126 (2008).
[18] S. Bleher, C. Grebogi, and E. Ott, Physica D **46**, 87 (1990).
[19] G. Contopolous, H. E. Kandrup, and D. Kaufman, Physica D **64**, 310 (1993).
[20] M. Zaslavsky, *Chaos in Dynamical Systems* (Harwood, New York, 1985); *Physics of Chaos in Hamiltonian Systems* (Imperial College Press, London, 1998).
[21] C. Grebogi, E. Ott, and J. A. Yorke, Physica D **7**, 181 (1983); S. Bleher, C. Grebogi, E. Ott, and R. Brown, Phys. Rev. A **38**, 930 (1988); S. Bleher, C. Grebogi, and E. Ott, Physica D **46**, 87 (1990).

[22] K. T. Alligood, T. D. Sauer, and J. A. Yorke, *Chaos, An Introduction to Dynamical Systems* (Springer-Verlag, New York, 1997).
[23] T. Tel, in *Directions in Chaos*, edited by Bai-lin Hao (World Scientific, Singapore, 1990), Vol. 3.
[24] E. Ott, *Chaos in Dynamical Systems* (University of Cambridge, Cambridge, UK, 1992).
[25] T. Tel and M. Gruiz, *Chaotic Dynamics* (Cambridge University Press, Cambridge, UK, 2006).
[26] P. Curie, J. Phys. Theor. Appl. **3**, 393 (1894).
[27] P. Reimann, Phys. Rep. **361**, 56 (2002).
[28] A. J. Lichtenberg and M. A. Lieberman, *Regular and Chaotic Dynamics* (Springer-Verlag, New York, 1983).